Measurements on an Oscillating 70-Deg Delta Wing in Subsonic Flow

M. R. Soltani* and M. B. Bragg†
The Ohio State University, Columbus, Ohio
and
J. M. Brandon‡
NASA Langley Research Center, Hampton, Virginia

A series of low-speed wind tunnel tests on a 70-deg sharp leading-edged delta wing at both static and dynamic conditions were performed to investigate the aerodynamic forces and moments. Forces and moments were obtained from a six-component internal strain-gauge balance. Large amplitude dynamic motion was produced by sinusoidally oscillating the model over a range of reduced frequencies. Static results compared well with previous experimental findings. Significant Reynolds number effects were present in the experimental measurements. Reynolds number effects are reduced, but still present when a sharper leading-edge delta wing was tested. Large hysteresis loops and a delay in dynamic stall were seen in the dynamic data. Dynamic forces and moments were a strong function of reduced frequency. Nonzero sideslip created complex rolling moment and lift behavior due to asymmetric vortex bursting.

Nomenclature

C_D = drag coefficient
C_L = lift coefficient
$C_{L\alpha}$ = variation of lift coefficient with angle of attack (/deg)
C_M = pitching-moment coefficient
$C_{M\alpha}$ = variation of pitching moment coefficient with angle of attack (/deg)
C_N = normal-force coefficient
C_l = rolling-moment coefficient
c = wing root chord (ft)
f = frequency (Hz)
k = reduced frequency $\pi fc/U_\infty$
R_e = Reynolds number based on the root chord
U_∞ = tunnel speed (ft/s)
α = angle of attack (deg)
β = sideslip angle (deg)
Λ = wing sweep

Introduction

SINCE the early use of aircraft in combat, a consistent demand for greater maneuverability has played a major role in the design of fighter aircraft.[1,3] A high angle of attack and poststall flight at high pitch rates has proven to be a great advantage.[1] As a result, current and future fighter aircraft design trends are in favor of abandoning angle of attack limitations in low-speed flight.[4] The use of highly swept, slender, sharp-leading-edge delta wings, or variations of this planform, are common among high performance aircraft. These swept wings have desirable low drag characteristics at high speed and good high angle of attack characteristics at low speed.

Flow visualization on delta wings[5,6] has shown one lift producing mechanism to be a pair of strong leading-edge vortices formed on the upper surface. These vortices induce additional velocities on the suction surface of the wing producing additional lift referred to as vortex lift.[7] The stall of delta wings is caused by the breakdown of the vortices on the wing, which leads to a reduction in the nonlinear, vortex-induced lift.[5,8] Wentz[9] and McKernan and Nelson[10] correlated static force measurements to flow visualization to show the relationship between leading-edge vortex formation and bursting and the forces and moments on the wing. Flow visualization with flowfield measurements of the vortex field[11-13] provide additional insight into the delta wing at a high angle of attack.

Some researchers have explored other aspects of static, vortical flowfields. Reynolds number and Mach number effects were studied by Shrader et al.,[14] and Shi et al.[15] considered Reynolds number effects in his study of jet blowing on delta wings. Sideslip effects on delta wings have been studied extensively by Verhaagen[16] and Verhaagen and Naarding.[17] Verhaagen used flow visualization, surface pressure measurements, and balance-generated force and moment data to provide insight into the asymmetric effects due to sideslip. Verhaagen's data, however, are limited to angles of attack less than 25 deg. More realistic fighter aircraft configurations have been tested at high angles of attack yielding results, qualitatively similar to the delta wing studies.[3,17,18]

The research reviewed above was for high angles of attack but under static conditions. However, high-performance aircraft usually experience a high angle of attack at high angular velocity. Recently, research has focused on delta wings at high angles of attack undergoing pitch oscillations. Flow visualization has shown a hysteresis in the measured vortex burst location, which depends on the pitch oscillation frequency and amplitude.[8,20-24] Wolffelt[23] shows hysteresis loops in the normal force and pitching moment data, which correlate to the movement of the vortex burst point.

Therefore, until 1988, to the author's knowledge, the only measured force and moment data for delta wings oscillating in pitch at a high angle of attack were that of Wolffelt.[23] Since then, Cunningham,[25] Naumowicz, Brandon and Shah,[27] and Soltani et al.[28] have all reported force and moment data on oscillating delta wings. The research summarized here is part of this recent effort to study the forces and moments and correlate them to the flow visualization data.[28] Since a significant amount of flow visualization data are available in the literature for a pitching 70-deg delta wing, this paper does not repeat that work. Instead, the objective here is to study the effect of oscillation frequency, sideslip, and Reynolds number

Presented as Paper 88-2576 at the AIAA 6th Applied Aerodynamic Conference, Williamsburg, VA, June 6-8, 1988; received July 6, 1988; revision received Sept. 8, 1989.

*Graduate Research Assistant, Department of Aeronautical and Astronautical Engineering. Member AIAA.
†Associate Professor, Department of Aeronautical and Astronautical Engineering; currently at the University of Illinois, Urbana, IL. Senior Member AIAA.
‡Aerospace Engineer, Flight Dynamics Branch. Member AIAA.

on the forces and moments of a delta wing oscillating in pitch from 0- to 55-deg angles of attack.

Experimental Procedure

The experiments were conducted in the subsonic wind tunnel of Ohio State University located at the Aeronautical and Astronautical Research Laboratory. The tunnel-test section is approximately 5 ft wide, 3 ft high, and 8 ft long, and operates at speeds from 0 to 200 ft/s at a Reynolds number of up to 1.3×10^6 per foot. The tunnel is of open return type and uses four large antiturbulence screens and honeycomb to attain a turbulent intensity of less than 0.1%.

Model

The model was a simple flat plate delta wing of 70-deg leading-edge sweep, a 20.61-in. root chord and a 15-in. span at the trailing edge. The wing was constructed of 1/2 in.-thick plywood (0.024 thickness to chord ratio) and had sharp beveled leading and trailing edges. A pod large enough to house the balance and necessary hardware was attached under the wing. A drawing of the model used in this investigation is shown in Fig. 1.

Oscillation System

A system was designed to pitch the models through large amplitude oscillations. The oscillation system uses a belt and pulley reduction system to obtain oscillation frequencies of 0 to 2.3 Hz. The last pulley in the system drives a cam that produces a sinusoidal pitching motion of the model from 0 to 55-deg angles of attack. The present system also allows sinusoidal pitching motion at steady sideslip angles to ± 15 deg in increments of ± 5 deg. A potentiometer mounted on the arm of the oscillation system provides the instantaneous angle of attack of the model. The delta wing model was pitched about the 57% root-chord location. The z-location of the pitch axis was about 0.15 c below the wing chord line.

Force Measurement

Force measurements were made using a six-component internal strain gauge balance. There are two types of tares that must be subtracted from the measured forces and moments. The first are the gravitational loads due to the model and balance weight, which are functions of the angle of attack. The second are the inertial forces and moments produced by the moments of inertia of the oscillating model and balance. The magnitude of the tares was calculated in a straightforward manner based on geometry and oscillation frequency. From experimental measurements, it was found that the internal strain-gauge balance itself made a considerable contribution to these tares. After removing the balance-alone tares from those of the balance with the model installed, the calculated tares compared very well with the measured ones. These comparisons indicate that the effect of the surrounding still air on the model as it oscillates, wind off, is negligible. These tares were curve fit for each case as a function of the angle of attack using a polynomial and later were subtracted from the measured loads.

Data Acquisition and Reduction

Data were taken and reduced on an IBM PC/AT with a 12-bit, 16-channel analog to digital board. Dynamic data presented in this paper were digital filtered, then averaged over several cycles. Aerodynamic forces and moments were measured at the balance moment center and have been transferred to the 25% wing root-chord station. All moments were nondimensionalized with respect to 2/3 wing root chord. Longitudinal forces and moments are in the wind-axis system, and lateral-directional forces and moments are in the body-axis system.[29]

Blockage corrections at small angles of attack were estimated by the method of Ref. 29 and were found to be small. In addition Ref. 30 suggests that blockage ratios of less than 7% can usually be considered negligible. The blockage ratio for this investigation was 6%. Thus no correction has been applied to the data.

Results and Discussion

In Fig. 2 the measured static variation of the lift coefficient with the angle of attack is compared to theory and other experiments. The nonlinearity in lift with the angle of attack is quite clear. This nonlinearity is a result of the coupling of the potential flow at a low angle of attack with the vortex lift generated by the delta wing geometry at moderate to high incidence. This phenomenon is clear from Fig. 2 when the experimental data are compared with the predicted values of the lift coefficient using the potential flow and the method of Polhamus.[7] Note that for small incidence, the experimental data compare well with the predicted potential flow lift. The experimental results are in good agreement with Polhamus' theory of Ref. 7 until near the angle for maximum lift.

Large deviation between the experimental and theoretical values above an incidence of 28 deg are caused by the bursting phenomenon, which was not considered in the theory of Polhamus.[7] In Fig. 3, the lift curve slope is plotted vs the angle of attack for the 1 million Reynolds number case. The angle of attack at which flow visualization has shown the vortex burst point reaching the delta wing trailing edge[9,10,19] are indicated

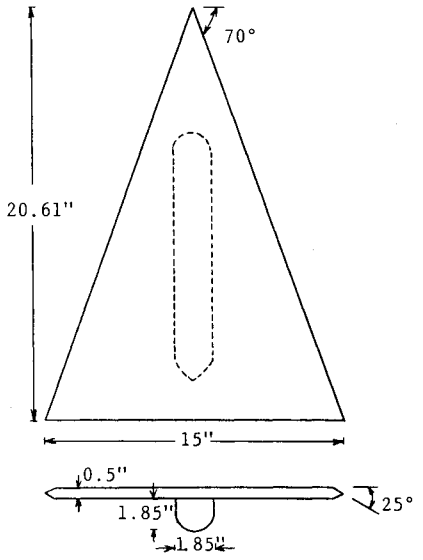

Fig. 1 The delta wing model (dimensions are in inches).

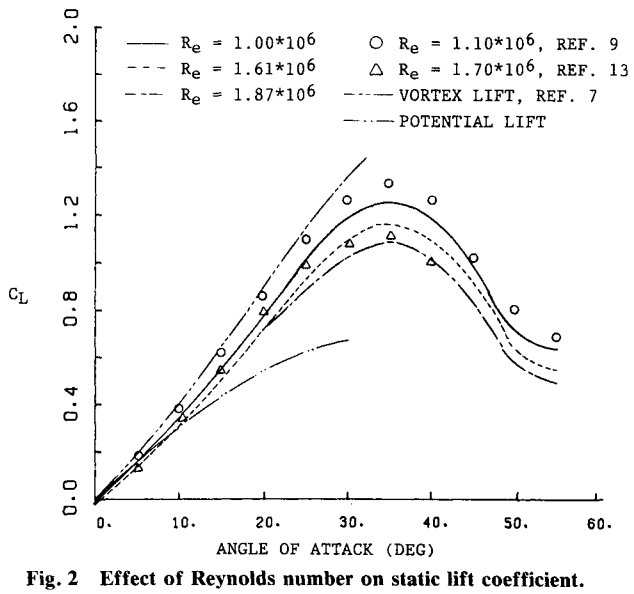

Fig. 2 Effect of Reynolds number on static lift coefficient.

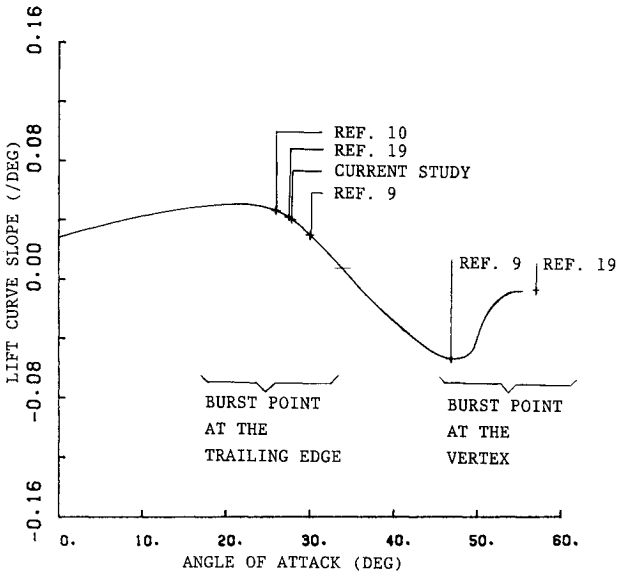

Fig. 3 Static variation of the lift-curve slope with angle of attack ($Re = 1.0 \times 10^6$).

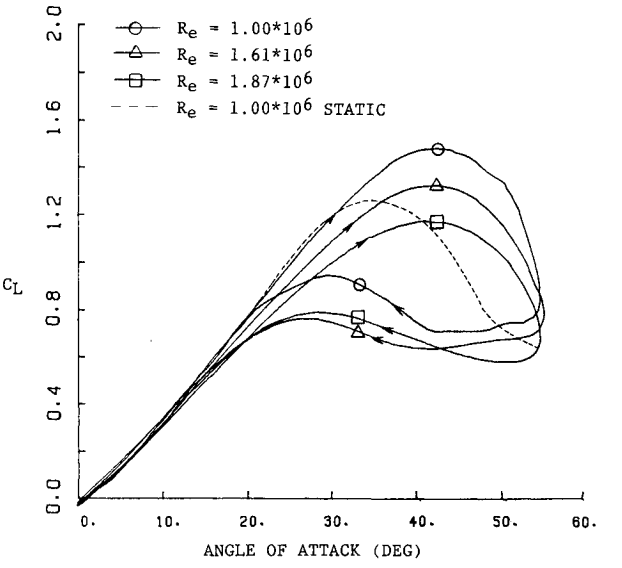

Fig. 4 Effect of Reynolds number on dynamic lift coefficient ($k = 0.035$).

on the figure. This includes current flow visualization results using a method similar to that of Brandon and Shah,[27] which shows the vortex burst point at the trailing edge at 28 deg angle of attack. The lift-curve slope increases demonstrating nonlinear vortex lift until the vortex burst point reaches the trailing edge. As the angle of attack is increased, the burst point progresses forward reducing the lift curve slope. When the slope is zero, at 36 deg angle of attack, maximum lift is reached.

The slope continues to decrease, as does the delta wing lift, as the angle of attack is increased further. At approximately 47 deg angle of attack, the lift-curve slope becomes a minimum. This is related to the vortex burst point reaching the vicinity of the leading edge. The angle of attack at which this first occurs is very difficult to determine from flow visualization. Skow et al.[19] reports this occurring at 60 deg. Brandon and Shah[27] reports the burst point occurring at $x/c = 0.05$ at an angle of attack of 40 deg. From this figure it is seen that the movement of the burst point over the wing significantly affects the model forces and moments. The relationship seen here can be used later to help describe the dynamic effects in forces and moments due to changes in burst point locations.

Reynolds Number Effects

The static lift coefficient measurements presented in Fig. 2 show a significant effect on Reynolds number. By comparing the present data at matched Reynolds number to that of Wentz[9] and Hummel and Srinivasan,[13] the data compare well. Here by decreasing the Reynolds number from 1.87 to 1.0 million, the maximum lift increases by 0.16. This is also seen in the dynamic data, see Fig. 4, where an even larger increase in maximum lift is obtained by reducing the model Reynolds number.

Polhamus[1] states that Reynolds number has little effect on delta wing lift. However, Reynolds number effects on the flowfield over a delta wing are well documented. Kjelgaard et al.[11] used surface oil flow to show the effect of boundary-layer transition on the secondary separation line. At a Reynolds number based on running length of 0.8×10^6 to 0.9×10^6, transition occurs, moving the secondary separation out toward the leading edge. Polhamus[1] discusses surface pressure measurements taken at chord Reynolds number of 1.6×10^6 and 6.4×10^6. These show large changes in the surface pressure depending on the state of the boundary layer. Shi et al.[15] measured a more forward vortex breakdown location with an increasing Reynolds number in the range of 1×10^4 to 5×10^4. Lemay et al.[24] saw a similar forward movement of the vortex point for an oscillating model during upstroke motion for Reynolds numbers from 0.175×10^6 to 0.26×10^6.

The large Reynolds number effects seen here may be a result of the way in which the model leading edge was sharpened, see Fig. 1. Elle[31] showed an effect on vortex position due to leading-edge shape, and Wolffelt[23] states that thicker wings may be more Reynolds number sensitive. In Fig. 5, Reynolds number effects on static lift for the much sharper and thinner aluminum wing[32] are shown compared to the current symmetric beveled wing. Here the two models and support system are identical except for the leading-edge geometry. Note that the aluminum wing of Ref. 32 is beveled up from the lower surface creating a negatively cambered wing and therefore negative lift at a zero-deg angle of attack. For the sharper aluminum wing, the effect of a Reynolds number appears to be restricted to angles of attack above 28 deg, where the burst point moves onto the wing. At maximum lift, the same trend is seen as in the symmetric beveled wing with a higher maximum lift as the Reynolds number is decreased. However, the effect of Reynolds number, though still present, is much less for the sharper wing. Therefore, for the Reynolds number range 1×10^6 to 1.87×10^6, the sharper leading edge delays Reynolds number effects to the higher angles of attack, but a significant effect of Reynolds number on maximum lift is still present.

Pitch Oscillation Effects

The 70-deg delta wing was sinusoidally oscillated in pitch from 0 to 55 deg angle of attack at reduced frequencies from 0.015 to 0.0815. In Figs. 6–9 the measured longitudinal forces and moments are shown at zero sideslip with varying reduced frequency at a Reynolds number of 1.61×10^6.

Figure 6 presents the normal force coefficient vs angle of attack for three reduced frequencies. Static data are also plotted as a baseline. For $k = 0.015$, the value of $C_{N\alpha}$ starts to decrease at an angle of about 30 deg, whereas for the static case, this occurs at an angle of about 25 deg. This is an indication of the delay in separation and vortex bursting during the dynamic upward motion. Further increase in the incidence results in the vortex burst point moving forward onto the wing, thus reducing the vortex lift contribution to the normal force. As the reduced frequency is increased, the flow lag effect increases and results in the higher maximum C_N values.

In the downstroke motion, the flow starts reattaching from the wing apex and progresses toward the trailing edge. During

the downward motion for the $k = 0.015$ data, the variation of $C_{N\alpha}$ with alpha drops from a large positive value to its maximum negative value at an angle of about 42 deg. This indicates that the flow remains separated until an angle of 42 deg in downward motion. From here on, the leading-edge vortices start attaching to the suction side from the wing leading edge and proceed back to the trailing edge. At an angle of about 23–25 degrees, $C_{N\alpha}$ reaches the same value as it had in the upstroke motion. These differences in $C_{N\alpha}$ between upstroke and downstroke motion are caused by the flow lag effect, which creates the hysteresis loop. At a higher reduced frequency, the effect of the flow lag is more pronounced and produces a wider hysteresis loop with maximum normal force increasing and occurring at higher angles of attack.

Lemay et al.[24] performed flow visualization on a 70-deg delta wing oscillation from 0 to 45 deg angle of attack. Vortex burst point locations were recorded for reduced frequencies of 0.025 and 0.15. They noted a lag in burst point location relative to the static case on the upstroke and downstroke as is indicated by the measured normal force in Fig. 6. The lag was very large for the $k = 0.15$ case on the downstroke. This qualitatively compares well to Fig. 6, where the normal force on the downstroke shows a much larger hysteresis for the $k = 0.0815$ case as compared to the $k = 0.015$ case. Brandon and Shah[27] show normal force values that are somewhat lower; the increase in maximum C_N due to the oscillation is similar to Fig. 6 as is the shape of the hysteresis loop.

The dynamic variation of the lift coefficient with an angle of attack for various reduced frequencies is shown in Fig. 7. Comparison of the dynamic data with the static case at the same Reynolds number clearly shows an increase in maximum lift and delayed separation for all cases reported. Increasing the pitch rate has a significant influence on the dynamic stall angle that increases over 10 deg from the static value. Maximum lift overshoot did not vary significantly with reduced frequency in the range tested here.

Figure 8 shows the effect of reduced frequency on drag coefficient during large amplitude sinusoidal motion. A much higher drag is evident at a high angle for the pitch-up motion compared with the static case. While on the downstroke motion, the hysteresis in the dynamic drag curve shows substantial reduction in drag when compared to the static data. These variations in drag during up and down motions are probably due to the variations of the normal force discussed previously.

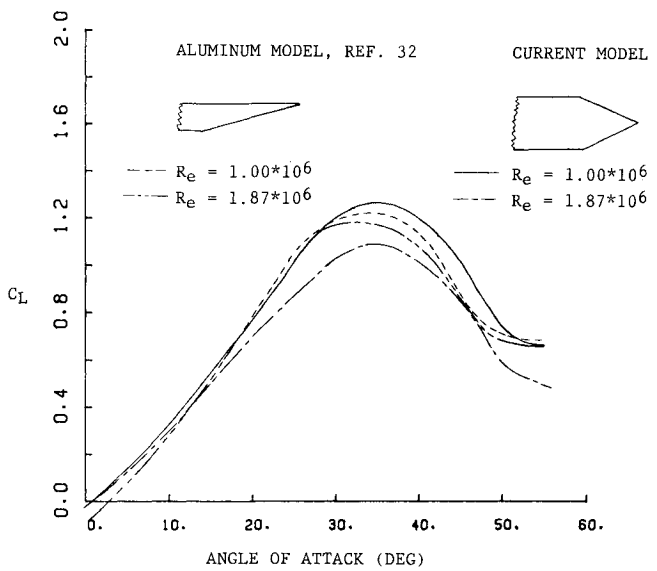

Fig. 5 The effect of Reynolds number on the static lift coefficient for two different delta wing models.

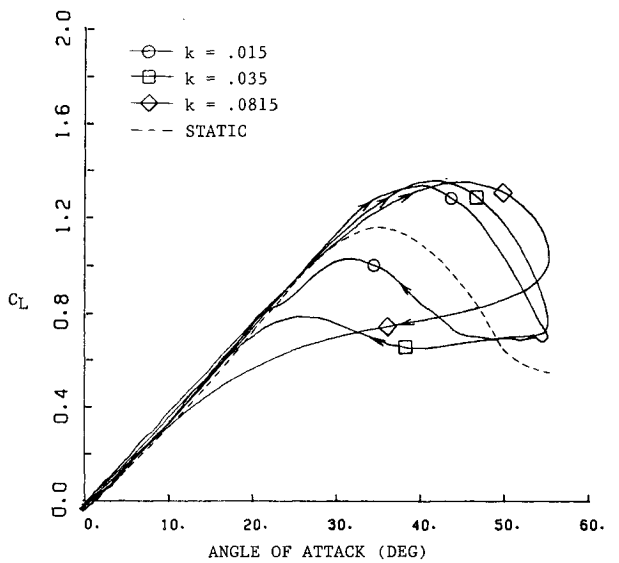

Fig. 7 Effect of reduced frequency on lift coefficient ($R_e = 1.61 \times 10^6$).

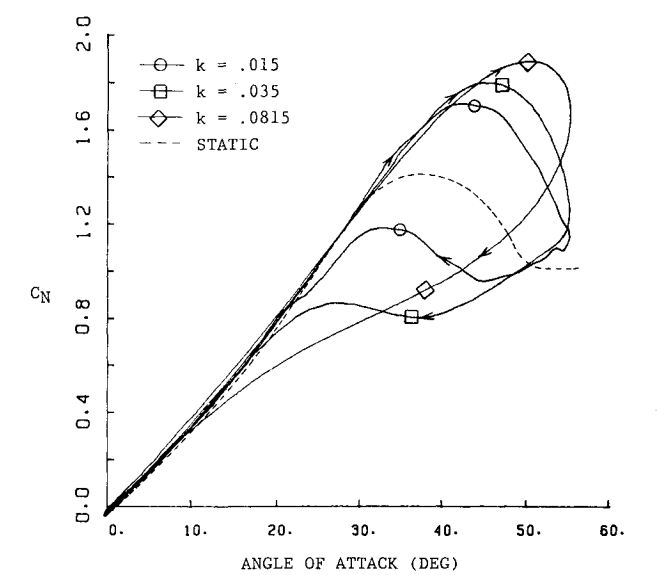

Fig. 6 Effect of reduced frequency on normal force coefficient ($R_e = 1.61 \times 10^6$).

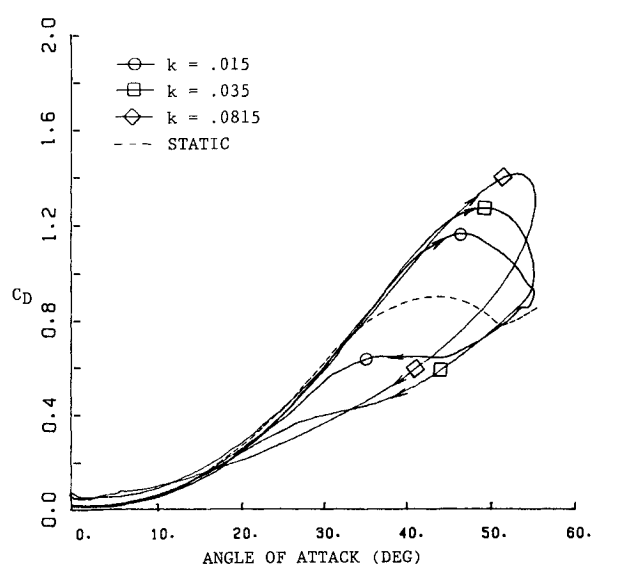

Fig. 8 Effect of reduced frequency on drag coefficient ($R_e = 1.61 \times 10^6$).

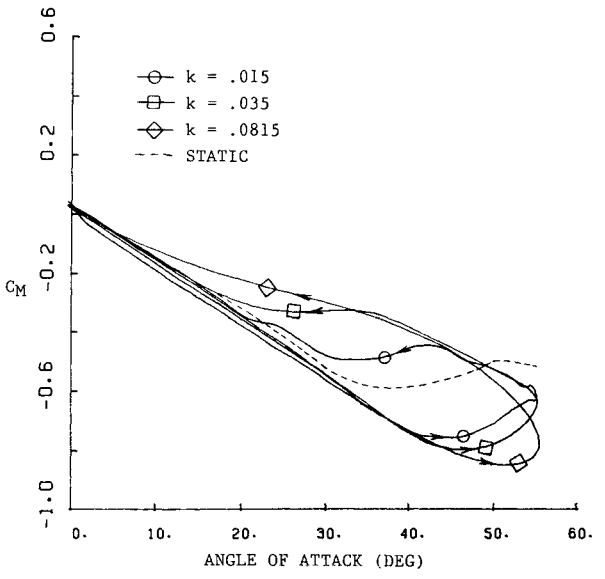

Fig. 9 Effect of reduced frequency on pitching moment coefficient ($R_e = 1.61 \times 10^6$).

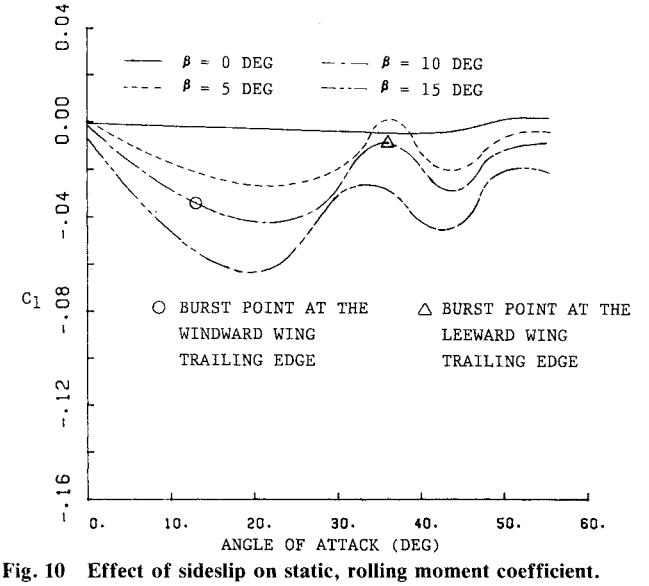

Fig. 10 Effect of sideslip on static, rolling moment coefficient.

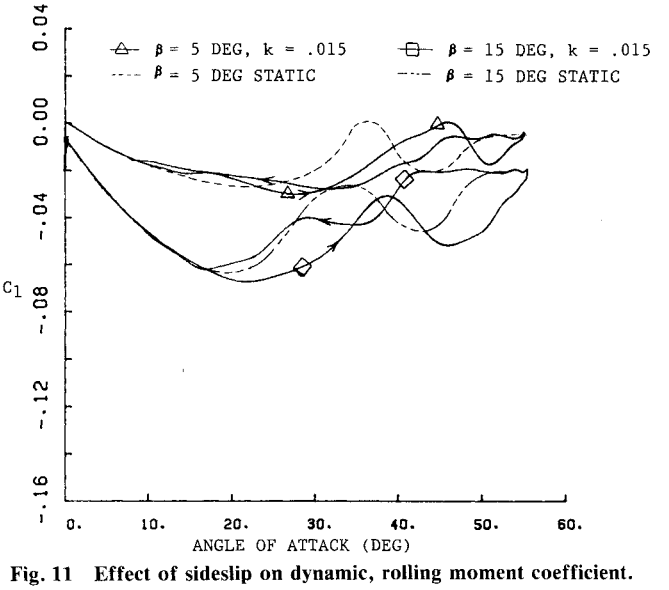

Fig. 11 Effect of sideslip on dynamic, rolling moment coefficient.

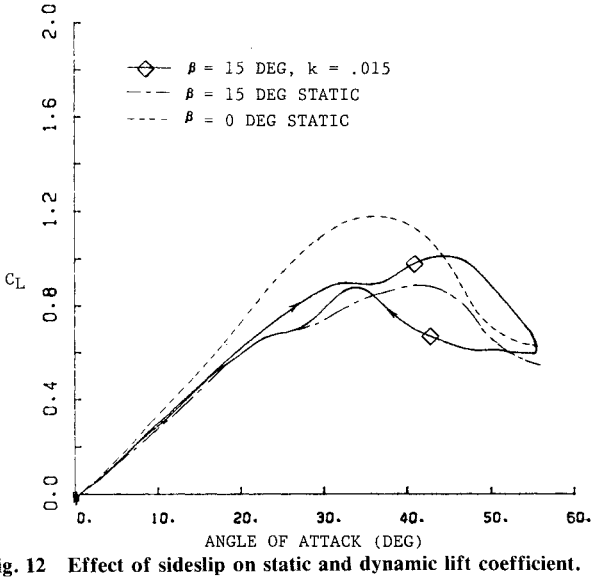

Fig. 12 Effect of sideslip on static and dynamic lift coefficient.

The influence of pitch rate on the character of drag force hysteresis loop and its magnitude is apparent.

Figure 9 shows the corresponding pitching moment data of the model for both the static and dynamic cases. Again, the influence of reduced frequency on the pitching moment hysteresis loop and its magnitude is apparent. On the upstroke, as the burst point crosses the trailing edge, $C_{M\alpha}$ becomes nonlinear with C_M becoming less negative. This point is a function of reduced frequency. Further increasing the incidence results in the loss of normal force and a change in the sign of $C_{M\alpha}$. During pitch-up motion, a much larger negative pitching moment is evident compared to the static value due to delay of vortex bursting, whereas on the downward motion, the dynamic pitching moment has a substantially smaller negative value due to a delay in reattachment.

Sideslip Effect

Figure 10 shows the static variation of the rolling moment coefficient with an angle of attack at several sideslip angles. The nonzero roll at zero sideslip is probably due to a slight model asymmetry or misalignment. At a nonzero sideslip angle, the effective sweep of the windward wing decreases and the sweep of the leeward wing increases. Asymmetrical vortex bursting then occurs where the burst points of the windward and leeward wing vortices reach the model at different angles of attack. This leads to a complex, highly nonlinear, rolling moment behavior with angle of attack.

For the $\beta = 10$-deg sideslip, initially the rolling moment decreases with an increasing angle of attack. In this angle of attack range, the windward vortex is stronger than the leeward vortex causing the negative rolling moment. If the windward wing vortex were to behave in a manner similar to a 60-deg delta wing at $\beta = 0$, the burst point would reach the trailing edge at an angle of attack of 18 deg.[19] Here our flow visualization shows, at the Reynolds number of 0.14×10^6 tested, that the burst point reaches the windward wing trailing edge at an angle of attack of 13 deg. As the angle of attack is increased further, the burst point moves up onto the wing on the windward side. With a further increase in angle of attack, lift is lost on the windward wing. The model generates a rolling moment to push the windward side down, a more positive rolling moment. Brandon and Shah,[27] McKernan and Nelson,[10] and John and Krause[3] have also seen this effect on delta wings and a fighter configuration, respectively.

A maximum is seen in the measured rolling moment for $\beta = 10$ deg at an angle of attack of 36 deg. This is related to the leeward wing burst point reaching the delta wing trailing edge. For an 80-deg delta wing at $\beta = 0$, this occurs at 38 deg angle

of attack,[19] and flow visualization on this model yields a 36-deg angle of attack. Also in this angle of attack range near the minimum rolling moment, the windward vortex burst point reaches the leading edge.

As the angle of attack is increased beyond 36 deg, the leeward wing vortex moves forward on the wing. This decreases the lift on the leeward side and results in a more negative rolling moment. The local minimum in rolling moment near an angle of attack of 43 deg is due to the leeward vortex burst point reaching the leading-edge region of the wing.[19,27] As the angle of attack is increased further, and the model flowfield approaches a completely separated state, the rolling moment approaches zero. The rolling moment behavior is a result of the changing lift force on the leeward and windward wings and can be seen in the measured lift or normal force. By examining the lift-curve slope with the angle of attack, as in Fig. 3, an argument similar to the one above can be made.[28]

The effect of sinusoidal oscillation at a constant sideslip angle on the rolling moment coefficient is shown in Fig. 11. Static and dynamic data at $k = 0.015$ are shown at sideslip angles of 5 and 15 deg. The primary effect of an oscillating angle of attack on rolling moment is a delay in the static characteristics. This delay is a result of vortex bursting.[27]

At 5 deg sideslip, the dynamic data follow the static values until approximately 25 deg angle of attack. Delay of the windward wing vortex burst point reaching the trailing edge is seen as a shift in the minimum value of rolling moment during the upstroke. The local maximum associated with the leeward vortex bursting crossing the trailing edge is also seen to lag during the dynamic motion. This point shifts from 36 deg angle of attack statically to 46 deg during the upstroke in dynamic motion. During the downstroke, the rolling moment is constant from 55 to 46 deg angle of attack as the vortices again form at the delta wing apex. As the angle of attack is reduced further, the rolling moment trends are similar to the upstroke. Brandon and Shah[27] show dynamic rolling moment data for a different oscillation frequency and amplitude, which are qualitatively similar to those shown here. Also shown in Fig. 11 are data at 15 deg sideslip. The results are similar to the 5 deg data in the upstroke. During the downstroke, the constant rolling moment region due to delayed vortex formation is quite extensive. Here it extends from 55 to 43 deg angle of attack. Continuing the downstroke, the lag in vortex formation and bursting leads to a rolling moment behavior similar to the upstroke but lagging by approximately 10 deg in angle of attack.

The effect of sideslip on lift coefficient is shown in Fig. 12. The static data at 15 deg of sideslip show a large reduction in lift compared to the no-sideslip static case. This is due to the loss of lift on the windward wing due to early vortex breakdown. The break in the lift curve slope at approximately 20 deg angle of attack is associated with the loss of lift on the windward wing. This compares well with the minimum in the rolling moment data seen in Fig. 11. Maximum lift is reduced and occurs at a higher angle of attack for the 15-deg sideslip case. This is consistent with the delay in the leeward wing vortex bursting. Maximum lift occurs at 41 deg angle of attack, which again compares well to the local minima in rolling moment at the same angle of attack.

Verhaagen[16] found similar effects on the longitudinal forces and moments with sideslip. A reduction in lift was measured due to the effect of the windward vortex burst point. This was also seen to correspond to a change in the rolling moment. Verhaagen presents only static data below 25 deg angle of attack; therefore further comparisons are not possible.

Oscillating the model in pitch at constant sideslip angle leads to a lag in the static effects of vortex bursting described above. The reduction in lift-curve slope due to windward wing vortex bursting is delayed 10 deg in angle of attack over the static value. Maximum lift during the upstroke is delayed in angle of attack and reaches a higher value in the dynamic case. Hysteresis between the downstroke and upstroke is clearly seen. Windward wing bursting lags the upstroke behavior significantly and occurs at a similar location to the static value. This is also noted in the rolling moment data during the downstroke, see Fig. 11.

Conclusions

The forces and moments on delta wings are highly dependent on the state of its vortical field. The nonlinear vortex lift and the movement of the burst point on the wing are related to changes in measured lift-curve slope. It is often assumed that the lift on sharp leading-edged delta wings are relatively Reynolds number insensitive. The lift measured on this delta wing with a symmetrically chamfered leading-edge was very sensitive to Reynolds number changes from 1 to 2 million. This sensitivity was found under both static and dynamic conditions. A thinner wing, chamfered up from the lower surface, was found to be less sensitive to a Reynolds number.

Pitch oscillation causes large overshoots and hysteresis loops in the measured forces and moments. These effects are found to be dependent on the reduced frequency. Maximum lift increases rapidly between the static value and a reduced frequency of 0.015. Little change in maximum lift is seen between $k = 0.015$ and 0.0825; although the angle of attack for maximum lift increases. The effect of pitch oscillation can be related to the delay in vortex bursting.

Lift and rolling moment measurements are highly nonlinear with nonzero sideslip. These effects correspond to the asymmetric vortex bursting induced by the sideslip. The lift and rolling moment are affected greatly by the delay in vortex bursting due to the reduced frequency of the oscillation.

Acknowledgment

This work was supported in part by grant NAG-1-641 from NASA Langley Research Center. The authors would like to thank Mark Ringer, Jim Negro, and Jeff Keip, undergraduate research assistants, for their help in acquiring and reducing the data for this report.

References

[1]Polhamus, E. C., "Vortex Lift Research: Early Contributions and Some Current Challenges," NASA CP 2416, Vol. I, 1986.

[2]Polhamus, E. C., "Applying Slender Wing Benefits to Military A/C," *Journal of Aircraft,* Vol. 21, No. 8, Aug. 1984.

[3]John, H. and Kraus, W., "High Angle of Attack Characteristics of Different Fighter Configurations," AGARD-CP-244, 1978, pp. 2-1-2-15.

[4]Brandon, J. M. and Nguyen, H. T., "Experimental Study of Effects of Fore-body Geometry on High Angle of Attack Static and Dynamic Stability," AIAA Paper 86-0331, Nov. 1985.

[5]Nelson, R. C., "The Role of Flow Visualization in the Study of High Angle of Attack Aerodynamics," *Tactical Missile Aerodynamics,* edited by M. J. Hemsch and J. N. Nielsen, Vol. 104, Progress in Astronautics and Aeronautics, AIAA, New York, 1986.

[6]Elle, B. J. and Jones, J. P., "A Note on the Vorticity Distribution on the Surface of Slender Delta Wing with Leading Edge Separation," *Journal of the Royal Aeronautical Society,* Vol. 65, March 1961, pp. 195-198.

[7]Polhamus, E. C., "Prediction of Vortex-Lift Characteristics by Leading-Edge Suction Analogy," *Journal of Aircraft,* Vol. 8, No. 4, 1971, pp. 193-199.

[8]Payne, F. M., "The Structure of Leading Edge Vortex Flows Including Vortex Breakdowns," Ph.D. Dissertation, Univ. of Notre Dame, Notre Dame, IN, 1987.

[9]Wentz, William H., "Wind Tunnel Investigations of Vortex Breakdown on Slender Sharp-Edged Wings," Ph.D. Dissertation, University of Kansas, Lawrence, KS, 1968.

[10]McKernan, J. F. and Nelson, R. C., "An Investigation of the Breakdown of the Leading Edge Vortices on a Delta Wing at High Angles of Attack," AIAA Paper 83-2114, Aug. 1983.

[11]Kjelgaard, S. D., Sellers, W. L., III, and Watson, R. P., "The Flowfield Over a 75 Degree Swept Delta Wing at 20.5 Degrees Angle of Attack," AIAA Paper 86-1775, June 1986.

[12]Payne, F. M., Ng, T. T., Nelson, R. C., and Schiff, L. B., "Visu-

alization and Wake Surveys of Vortical Flow over a Delta Wing," *AIAA Journal,* Vol. 26, No. 2, Feb. 1988, pp. 137-143.

[13]Hummel, D. and Srinivasan, P. S., "Vortex Breakdown Effects on the Low-Speed Aerodynamic Characteristics of Slender Delta Wings in Symmetrical Flow," *Journal of the Royal Aeronautical Society,* Vol. 71, April 1967, pp. 319-322.

[14]Schrader, K. F., Reynolds, G. A., and Novak, C. J., "Effect of Mach Number and Reynolds Number on Leading-Edge Vortices at High Angles of Attack," AIAA Paper 88-0122, Jan. 1988.

[15]Shi, Z., Wu, J. M., and Vakili, A. D., "An Investigation of Leading-Edge Vortices on Delta Wings with Jet Blowing," AIAA Paper 87-0330, Jan. 1987.

[16]Verhaagen, N. G., "Some Low-Speed Wind-Tunnel Experiments on a Sharp-Edged Delta Wing of Aspect Ratio 1, with and without Yaw," Rpt. LR-283, Aug. 1979.

[17]Verhaagen, N. G. and Naarding, S. H. J., "Experimental and Numerical Investigation of the Vortex Flow Over a Yawed Delta Wing," AIAA Paper 88-2563-CP, June 1988.

[18]Hall, R. M., "Influence of Fore-body Cross Sectional Shapes on Wing Vortex-Burst Locations," *Journal of Aircraft,* Vol. 24, No. 9, Sept. 1987, pp. 645-652.

[19]Skow, A. M., Tiriga, J. R., and Moore, W. A., "Forebody/Wing Vortex Interactions and Their Influence on Performance and Spin Resistance," AGARD-CP-247, No. 6, pp. 6-1-6-26.

[20]Gilliam, F., Wissler, J., Robinson, M., and Walker, J., "Visualization of Unsteady Separated Flow About a Pitching Delta Wing," AIAA Paper 87-0240.

[21]Gad-el-Hak, M. and Ho, C. M., "The Pitching Delta Wing," *AIAA Journal,* Vol. 23, No. 11, Nov. 1985, pp. 1660-1665.

[22]Gad-el-Hak, M. and Ho, C. M., "Unsteady Vortical Flow Around Three Dimensional Lifting Surfaces," *AIAA Journal,* Vol. 24, No. 5, May 1986, pp. 713-721.

[23]Wolffelt, K. W., "Investigation of the Movements of Vortex Burst Position with Dynamically Changing Angle of Attack for a Schematic Delta Wing in a Water Tunnel With Correlation to Similar Studies in a Wind Tunnel," AGARD-CP-4123, 1986, pp. 27-1-27-8.

[24]LeMay, S. P., Batill, S. M., and Nelson, R. C., "Leading Edge Vortex Dynamics on a Pitching Delta Wing," AIAA Paper 88-2559-CP, June 1988.

[25]Cunningham, A. M., Jr., "Unsteady Low-Speed Windtunnel Test of a Straked Delta Wing, Oscillating in Pitch," Air Force Wright Aeronautical Lab, Wright-Patterson AFB, OH, AFWAL-TR-87-3098, April 1988.

[26]Naumowicz, T, "Aerodynamic Investigation of Delta Wings with Large Pitch Amplitude," AIAA Paper 88-4332, Aug. 1988.

[27]Brandon, J. M. and Shah, G. H., "Effect of Large Amplitude Pitching Motions on the Unsteady Aerodynamic Characteristics of Flat-Plate Wings," AIAA Paper 88-4331-CP, Aug. 1988.

[28]Soltani, M. R., Bragg, M. B., and Brandon, J. M., "Experimental Measurements on an Oscillating 70-Degree Delta Wing in Subsonic Flow," AIAA Paper 88-2576-CP, June 1988.

[29]Rae, W. H., and Pope, A., *Low-Speed Wind Tunnel Testing,* 2nd ed., Wiley, New York, 1984.

[30]Pass, C. Q., "A Wake Blockage Correction Method for Small Subsonic Wind-Tunnels," AIAA Paper 87-0294, Jan. 1987.

[31]Elle, B. J., "An Investigation at Low Speed of the Flow near the Apex of Thin Delta Wings with Sharp Leading Edges," British Aeronautical Research Council, London, ARC R & M 3176, Vol. 1, 1958, pp. 391-409.

[32]Bragg, M. B. and Soltani, M. R., "An Experimental Study of the Effect of Asymmetrical Vortex Bursting on a Pitching Delta Wing," AIAA Paper 88-4334, Aug. 1988.